


RESEARCH ARTICLE | AUGUST 07 2019

Gate-tunable anomalous transverse voltage at the superconducting LaAlO₃/SrTiO₃ interface

Yuedong Yan; Laiming Wei ; Linhai Guo; Fan Zhang; Jiyan Dai; Changgan Zeng




Appl. Phys. Lett. 115, 061603 (2019)

<https://doi.org/10.1063/1.5113584>




CrossMark



The Beginner's Guide to Cryostats and Cryocoolers
A detailed analysis of cryogenic systems

[Download guide ▼](#)

 Lake Shore
CRYOTRONICS

Gate-tunable anomalous transverse voltage at the superconducting $\text{LaAlO}_3/\text{SrTiO}_3$ interface

Cite as: Appl. Phys. Lett. **115**, 061603 (2019); doi: [10.1063/1.5113584](https://doi.org/10.1063/1.5113584)

Submitted: 5 June 2019 · Accepted: 16 July 2019 ·

Published Online: 7 August 2019



View Online



Export Citation



CrossMark

Yuedong Yan,^{1,2} Laiming Wei,^{1,2}  Linhai Guo,^{1,2} Fan Zhang,³ Jiyan Dai,³ and Changgan Zeng^{1,2,a)}

AFFILIATIONS

¹International Center for Quantum Design of Functional Materials (ICQD), Hefei National Laboratory for Physical Sciences at the Microscale, and Synergetic Innovation Center of Quantum Information and Quantum Physics, University of Science and Technology of China, Hefei, Anhui 230026, China

²CAS Key Laboratory of Strongly-Coupled Quantum Matter Physics, and Department of Physics, University of Science and Technology of China, Hefei, Anhui 230026, China

³Department of Applied Physics, The Hong Kong Polytechnic University, Hong Kong 999077, China

^{a)}E-mail: cgzeng@ustc.edu.cn

ABSTRACT

An anomalous transverse voltage near the superconducting transition is observed at the $\text{LaAlO}_3/\text{SrTiO}_3$ heterointerface. In contrast to the normal Hall effects, the observed anomalous transverse voltage persists even at zero magnetic field and is an even function of the magnetic field. It also responds anisotropically to out-of-plane and in-plane magnetic fields. Due to the two-dimensional nature of this superconducting electron system, this anomalous transverse signal is highly tunable via electrostatic gating. Strikingly, the temperature dependence of this transverse voltage exhibits a gate-tunable sign reversal behavior and can even undergo multiple sign reversals. Thorough analyses indicate that the anomalous transverse signal can be largely attributed to the guided vortex motion in the two-dimensional superconducting system. Our findings not only reveal important aspects of vortex dynamics at the strongly correlated oxide interface but also may promote the development of electrically tunable vortex dynamics.

Published under license by AIP Publishing. <https://doi.org/10.1063/1.5113584>

Vortex dynamics in superconductors attract extensive interest due to their rich physics, such as vortex liquid or vortex glass phenomena.^{1,2} The anomalous transverse voltage that occurs near the superconducting transition is a key tool for studying vortex physics.^{3–9} This vortex motion-induced transverse voltage is usually an even function of the external magnetic field (B) and sometimes even appears at $B = 0$ T.^{8,9} Despite many years of devoted efforts, achieving a clear understanding of the anomalous transverse voltage remains an open challenge due to complicated interactions between vortices and the surrounding environment. Recent approaches toward exploring vortex physics have exploited diverse novel materials, such as iron-based superconductors and layered organic superconductors. These systems have distinctive properties which have afforded several new discoveries, as well as a more profound understanding of vortex dynamics,^{10–12} such as the slow vortex creep observed in iron-based superconductors with a strong pinning landscape.¹⁰

$\text{LaAlO}_3/\text{SrTiO}_3$ (LAO/STO), a typical perovskite oxide heterostructure,¹³ can form a two-dimensional electron system (2DES) at its interface^{14,15} due to the polar catastrophe¹⁶ or oxygen

vacancies.^{17,18} The 2DES can even exhibit superconductivity at low temperatures.¹⁹ To date, a spectrum of emerging physical phenomena has been observed in this 2DES, such as nonmonotonic superconducting critical temperature²⁰ and spin-orbit coupling^{21–24} responses to band filling, the coexistence of superconductivity and magnetism,^{25–28} as well as the electrically tunable disorder^{29,30} and tetragonal domain order.^{31–33} However, the interplay between vortices and these properties remains to be exploited. Very recently, it was discovered that a Bose insulator phase, arising from the condensation of vortices and Cooper pair localization, occurs at the (111)-oriented LAO/STO interface and can be effectively tuned by disorder.³⁴ Recent theoretical work predicts the emergence of the so-called quantum anomalous vortices around magnetic impurity ions in a superconductor with strong spin-orbit coupling. Such vortices may support robust Majorana zero-energy modes.³⁵ The 2DES at the LAO/STO interface possesses all of the necessary criteria for realizing the quantum anomalous vortex. Therefore, this 2D correlated oxide superconductor may serve as an effective platform for the wider exploration of vortex dynamics.

In this work, we report an anomalous zero-field transverse voltage observed near the superconducting transition in the LAO/STO (001) system. This transverse voltage can be largely ascribed to the guided vortex motion at the LAO/STO interface. Interestingly, a sign reversal of the transverse voltage can be induced by electrostatic gating.

High-quality five unit-cell LAO overlayers were grown on TiO₂-terminated STO (001) substrates via pulsed laser deposition with a KrF laser.²³ To obtain an atomically flat surface, the STO substrates were carefully etched in a buffered HF solution and then annealed at 950 °C for 2 h in an oxygen atmosphere. The temperature and oxygen pressure were maintained at 650 °C and 1.0×10^{-4} mbar throughout LAO film growth. The layer-by-layer growth was monitored *in situ* via reflection high energy electron diffraction (RHEED), as shown in Fig. 1(a). After growth, the LAO/STO was cooled to room temperature at the growth oxygen pressure. Atomic force microscopy (AFM) confirmed the presence of atomically flat terraces on the sample surface [the inset of Fig. 1(a)].

Transport measurements were conducted on the LAO/STO interfacial 2DES which was mechanically patterned into a standard Hall bar geometry.^{21,23} Ohmic electrode contacts were wire bonded to the 2DES via Al wires. The Ti/Au electrode was deposited on the back side of the STO substrate to allow for the application of a back-gate voltage (V_g). Transport measurements were executed at extremely low temperatures in an Oxford dilution refrigerator, with the magnetic field applied perpendicular/parallel to the 2DES. As shown in Fig. 1(b), the longitudinal and transverse voltages (V_{xx} and V_{xy}) were measured simultaneously at a d.c. current (I) of 200 nA. The longitudinal resistance (R_{xx}) was obtained directly from $R_{xx} = V_{xx}/I$. Due to inevitable misalignment of the transverse contacts, the measured transverse voltage includes a small contribution from the longitudinal

component. Therefore, the transverse resistance (R_{xy}) is obtained by subtracting the scaled longitudinal resistance, i.e., $R_{xy} = (V_{xy} - AV_{xx})/I$, where the constant A is set to make $R_{xy} = 0$ in the normal conducting state.³⁶

Figure 1(c) shows R_{xx} and R_{xy} as functions of temperature at zero magnetic field. As the temperature (T) decreases, a nonzero R_{xy} emerges near the superconducting critical temperature (~ 290 mK) and then vanishes with further decreasing temperature. Moreover, the perpendicular magnetic field dependence of R_{xx} and R_{xy} [Fig. 1(d)] demonstrates that the transverse resistance appears around the superconducting critical field and is an even function of the magnetic field. As is well known, a zero-magnetic-field transverse voltage can be induced by the anomalous Hall effect in ferromagnetic materials.³⁷ However, the observed transverse resistance possesses even-in-field character and is correlated with superconductivity, neither of which is consistent with the anomalous Hall effect. The zero-field transverse resistance around the superconducting transition can be induced by three possible effects: the transverse inhomogeneity of superconductivity,³⁸ the electronic nematicity,³⁹ and the guided vortex motion.⁸

The trademark of an inhomogeneity-induced transverse signal is that R_{xy} should be proportional to dR_{xx}/dT .^{38,40} Figure 2 plots dR_{xx}/dT and R_{xy} vs temperature for varied out-of-plane and in-plane magnetic fields below the superconducting critical fields for $V_g = 0$ V. R_{xy} and dR_{xx}/dT exhibit a nearly identical temperature dependence at zero field. However, increasing the out-of-plane field causes the peak position of the R_{xy} - T curve to decrease more rapidly than that of the dR_{xx}/dT - T curve [Figs. 2(a) and 2(b)]. Moreover, increasing the in-plane field prompts a rapid decay to the peak magnitude of the dR_{xx}/dT - T curve, whereas that of the R_{xy} - T curve remains nearly unaffected [Figs. 2(c) and 2(d)]. Such deviations from proportionality between dR_{xx}/dT and R_{xy} suggest that the anomalous transverse resistance is not dominated by the spatial inhomogeneity of superconductivity. Figure 2 also shows that the parallel and perpendicular field transport measurements have significantly different magnetic field scales. This is because in such a two-dimensional superconducting system, the parallel critical magnetic field is revealed to be much larger than the perpendicular critical magnetic field.⁴¹

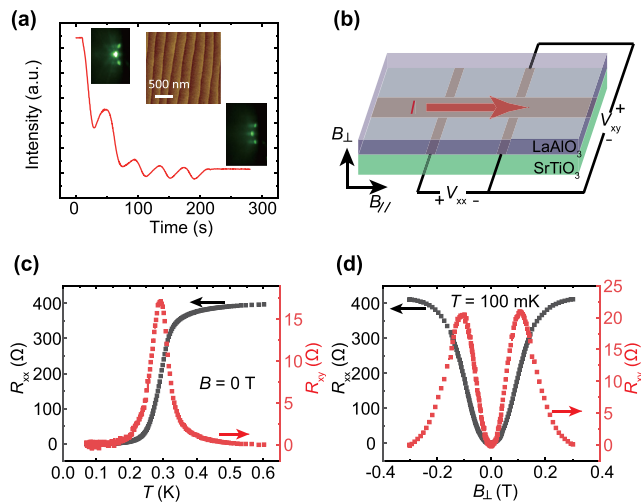


FIG. 1. (a) RHEED oscillations for growing the LAO film on the STO (001) substrate. The left and right insets are the RHEED patterns before and after growth, respectively, and the center inset is an AFM image of the LAO surface. (b) Schematic of the mechanically patterned Hall bar geometry of the LAO/STO interfacial 2DES for transport measurements. The transport channel is about 500 μ m wide. (c) R_{xx} and R_{xy} vs temperature at zero magnetic field. (d) R_{xx} and R_{xy} vs perpendicular magnetic field at $T = 100$ mK. The gate voltage is fixed at 0 V.

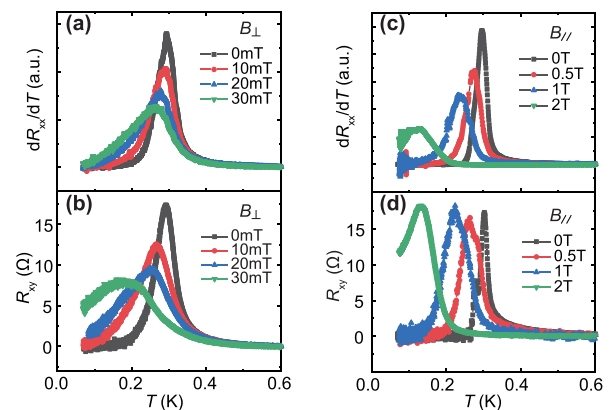


FIG. 2. (a) and (b) Temperature dependence of dR_{xx}/dT (a) and R_{xy} (b) at various perpendicular fields. (c) and (d) Temperature dependence of dR_{xx}/dT (c) and R_{xy} (d) at various parallel fields. The gate voltage is fixed at 0 V.

A recent report demonstrated that electronic nematicity-induced breaking of spontaneous rotational symmetry in copper oxide superconductors can yield a zero-field transverse voltage.³⁹ Theoretical studies predict that such nematic order can appear at the LAO/STO interface near the band edge of the d_{xz} and d_{yz} subbands,⁴² i.e., in the vicinity of the Lifshitz transition.⁴³ As shown in Figs. 3(a) and 3(b), the superconducting critical temperature first rises and then declines as the gate voltage is swept from negative to positive, which is consistent with previous reports.^{20,43} According to the experimental observation⁴³ and band structure calculations,^{44,45} the peak of this superconducting dome occurs near the Lifshitz transition. However, nonzero R_{xy} persists even for gate voltages far from this peak, as depicted in Figs. 3(b) and 3(c). Therefore, the zero-field transverse resistance cannot be attributed to the electronic nematicity.

Consequently, we ascribe the zero-field transverse resistance to the guided vortex motion. With decreasing temperature, the 2DES undergoes a Berezinskii-Kosterlitz-Thouless (BKT) transition^{46,47} to the superconducting state (see Fig. S1 in the [supplementary material](#) for details). According to the BKT model, free vortices can form due to the thermodynamic instability-induced unbinding of the vortex-antivortex pairs above the BKT transition temperature (T_{BKT}). The flow of an electric current in the superconductor causes the free vortex (antivortex) to experience a Lorentz force $F_L = J \times \phi_0$, where J is the current density and ϕ_0 is the flux carried by the vortex (antivortex). This driving Lorentz force can propel the vortex and antivortex in directions perpendicular to the current and opposite each other, as shown in Fig. 3(d). According to the Josephson relation,⁴⁸ the velocity (v) of vortex (antivortex) motion induces an electric field $E = -nv \times \phi_0$ [Fig. 3(d)], where n is the density of vortices. Since the induced electric fields are parallel to the current, the transverse voltage does not appear. However, when the superconductor contains an anisotropic pinning potential such as a linear pinning channel [see Fig. 3(e)], the vortices (antivortices) favor movement along the

pinning channel due to the guiding force. If such a channel is not perpendicular to the current, the guided motion of vortices and antivortices generates identical transverse electric-field components, whose direction is independent of the magnetic field direction.⁸ As a result, the guided vortex motion yields a transverse voltage which is an even function of the magnetic field, as confirmed by our experiments [Fig. 1(d)]. Figure S1 in the [supplementary material](#) shows that T_{BKT} is about 255 mK at $V_g = 0$ V. When the temperature decreases below this T_{BKT} , the complete binding of vortices and antivortices will cause R_{xx} and R_{xy} to vanish simultaneously. Our observation is consistent with this picture, as shown in Fig. 1(c).

As is well known, the STO experiences a ferroelastic transition from a cubic to tetragonal crystal structure when the temperature decreases to ~ 105 K.⁴⁹ This can generate striped tetragonal domain walls at the LAO/STO interface, which have been observed via a scanning superconducting quantum interference device,³¹ scanning charge detector,³² and scanning electron microscope.³³ It was shown in Ref. 32 that high negative gate voltages can remove the domain walls, and the change to the domain landscape remains even when the gate voltage is swept back to zero. However, we note that the results from another group (Ref. 33) are contrary to that in Ref. 32, that is to say, the gate voltage cycling can create more domain walls. As discussed in Ref. 32, the domain dynamics should depend on the sample growth condition and the patterned features of devices, which may explain the different observations in Refs. 32 and 33. In our experiments, the gate voltage cycling as shown in Fig. 4(a) remarkably enhances the transverse signal [see Figs. 4(b)–4(e)]. The enhancement suggests that the ferroelastic domain walls may provide a guiding force for vortex motion to induce the observed transverse voltage, and more domain walls are created after the gate voltage cycling, which is in agreement with the observation in Ref. 33. In addition, Figs. 4(b) and 4(d) show that the thermal cycling has a relatively small effect on the transverse signal, compared with the gate voltage cycling. The domain landscape may be changed by the thermal cycling. However, on the large measurement scale which is much larger than the domain size, the statistically averaged direction and density of domain walls may not be substantially affected by the thermal cycling,³¹ which explains the tiny dependence of the transverse voltage on the thermal cycling.

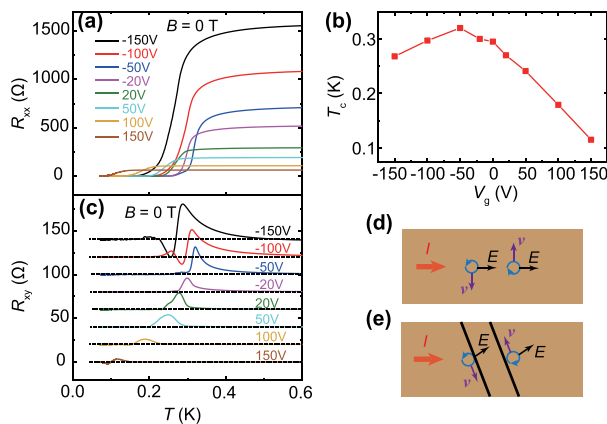


FIG. 3. (a) R_{xx} as a function of temperature at different V_g s in the absence of magnetic field. (b) T_c as a function of V_g . T_c is defined as the temperature where R_{xx} is half the normal-state resistance. (c) R_{xy} as a function of temperature at various V_g s after subtracting the longitudinal component. The curves are shifted vertically for clarity. The dashed lines indicate the reference lines where $R_{xy} = 0$. (d) and (e) Schematic of the vortex and antivortex motions without (d) and with (e) a pinning channel. I is the transport current, v is the velocity of vortex (antivortex) motion, and E is the electric field induced by the vortex (antivortex) motion.

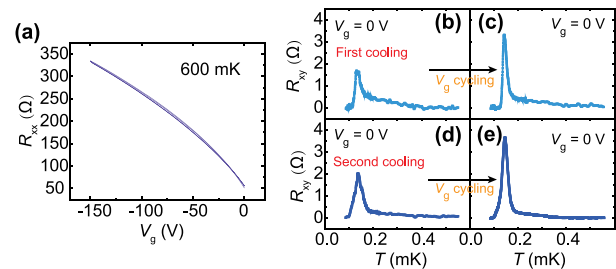


FIG. 4. (a) V_g -dependent R_{xx} of the as-cooled sample (cooling from 300 K at $V_g = 0$ V). V_g is swept back and forth between 0 V and -150 V. (b) Temperature-dependent R_{xy} at $V_g = 0$ V after the first cooling from 300 K to low temperature. (c) Temperature-dependent R_{xy} at $V_g = 0$ V after gate voltage cycling as shown in (a). (d) Temperature-dependent R_{xy} at $V_g = 0$ V after thermal cycling to 300 K and then back to low temperature. (e) Temperature-dependent R_{xy} at $V_g = 0$ V after the second cooling and gate voltage cycling.

Interestingly, the anomalous transverse signal can be effectively tuned by the gate voltage because of the 2D nature of the electron system and the high dielectric constant of the STO substrate [see Figs. 3(c) and S2 in the supplementary material]. Figure 3(c) reveals a remarkable nonmonotonically gate-tunable sign reversal behavior of R_{xy} . For $-100\text{ V} < V_g < 100\text{ V}$, R_{xy} near the superconducting transition is observed to be consistently positive. However, for $V_g \geq 100\text{ V}$, decreasing the temperature surprisingly prompts the sign of R_{xy} to change from positive to negative. Furthermore, for $V_g \leq -100\text{ V}$, R_{xy} undergoes sign reversal twice. Sign reversal behavior of the zero-field transverse voltage has also been observed in some bulk superconducting systems,^{36,50} but its physical origin is still unclear.

The LAO/STO 2DES has a wealth of noteworthy nonmonotonically gate-tunable physical properties. For example, the superconducting critical temperature exhibits clear dome-like behavior^{20,43} with a maximal value around -50 V as displayed in Fig. 3(b). In addition, it has been demonstrated that the spin-orbit coupling^{21–24} and the temperature range of superconducting phase fluctuation³⁰ in the 2DES also exhibit a nonmonotonic gate dependence. The anomalous gate-tunable sign reversal behavior reported in this present work may be intrinsically correlated with these nonmonotonic properties. Further efforts will be necessary to clarify this issue in the future.

In summary, we have observed an anomalous transverse voltage near the superconducting transition at the LAO/STO interface. This transverse signal can be ascribed to guided vortex motion, which may arise from the coupling between vortices and striped tetragonal domain walls. Moreover, the gate voltage can substantially tune such transverse voltage, even to the point of exhibiting sign reversal behavior. Therefore, the LAO/STO 2DES may offer an ideal platform to achieve electrostatic-tunable vortex dynamics for developing novel electronic devices.

See the supplementary material for the measurements about BKT transition and the temperature-dependent transverse voltage at various gate voltages before subtracting the longitudinal component.

This work was supported in part by the National Natural Science Foundation of China (Grant No. 11434009), the National Key R&D Program of China (Grant No. 2017YFA0403600), the Hefei Science Center CAS (Grant No. 2018HSC-UE014), the Anhui Initiative in Quantum Information Technologies (Grant No. AHY170000), and the Anhui Provincial Natural Science Foundation (Grant No. 1708085MF136). Jiyan Dai acknowledges support from the Hong Kong RGC Research Scheme (No. PolyU153000/18P).

REFERENCES

- G. Blatter, M. V. Feigel'man, V. B. Geshkenbein, A. I. Larkin, and V. M. Vinokur, *Rev. Mod. Phys.* **66**, 1125 (1994).
- W.-K. Kwok, U. Welp, A. Glatz, A. E. Koshelev, K. J. Kihlstrom, and G. W. Crabtree, *Rep. Prog. Phys.* **79**, 116501 (2016).
- A. T. Dorsey and M. P. A. Fisher, *Phys. Rev. Lett.* **68**, 694 (1992).
- T. Nagaoka, Y. Matsuda, H. Obara, A. Sawa, T. Terashima, I. Chong, M. Takano, and M. Suzuki, *Phys. Rev. Lett.* **80**, 3594 (1998).
- I. Puica, W. Lang, W. Göb, and R. Sobolewski, *Phys. Rev. B* **69**, 104513 (2004).
- N. Nakai, N. Hayashi, and M. Machida, *Phys. Rev. B* **83**, 024507 (2011).
- G. Zechner, W. Lang, M. Dosmailov, M. A. Bodea, and J. D. Pedarnig, *Phys. Rev. B* **98**, 104508 (2018).
- I. Janeček and P. Vašek, *Physica C* **390**, 330 (2003).
- V. Moshchalkov, R. Woerdenweber, and W. Lang, *Nanoscience and Engineering in Superconductivity* (Springer, 2010).
- S. Eley, M. Miura, B. Maiorov, and L. Civalé, *Nat. Mater.* **16**, 409 (2017).
- A. Fente, W. R. Meier, T. Kong, V. G. Kogan, S. L. Bud'ko, P. C. Canfield, I. Guillamón, and H. Suderow, *Phys. Rev. B* **97**, 134501 (2018).
- S. Uji, Y. Fujii, S. Sugiura, T. Terashima, T. Isono, and J. Yamada, *Phys. Rev. B* **97**, 024505 (2018).
- Y.-Y. Pai, A. Tylan-Tyler, P. Irvin, and J. Levy, *Rep. Prog. Phys.* **81**, 036503 (2018).
- A. Ohtomo and H. Y. Hwang, *Nature* **427**, 423 (2004).
- S. Thiel, G. Hammerl, A. Schmehl, C. W. Schneider, and J. Mannhart, *Science* **313**, 1942 (2006).
- N. Nakagawa, H. Y. Hwang, and D. A. Muller, *Nat. Mater.* **5**, 204 (2006).
- W. Siemons, G. Koster, H. Yamamoto, W. A. Harrison, G. Lucovsky, T. H. Geballe, D. H. A. Blank, and M. R. Beasley, *Phys. Rev. Lett.* **98**, 196802 (2007).
- G. Herranz, M. Basletić, M. Bibes, C. Carrétero, E. Tafrá, E. Jacquet, K. Bouzehouane, C. Deranlot, A. Hamzic, J.-M. Broto, A. Barthélémy, and A. Fert, *Phys. Rev. Lett.* **98**, 216803 (2007).
- N. Reyren, S. Thiel, A. D. Caviglia, L. F. Kourkoutis, G. Hammerl, C. Richter, C. W. Schneider, T. Kopp, A.-S. Rüetschi, D. Jaccard, M. Gabay, D. A. Muller, J.-M. Triscone, and J. Mannhart, *Science* **317**, 1196 (2007).
- D. Caviglia, S. Gariglio, N. Reyren, D. Jaccard, T. Schneider, M. Gabay, S. Thiel, G. Hammer, J. Mannhart, and J.-M. Triscone, *Nature* **456**, 624 (2008).
- H. Liang, L. Cheng, L. Wei, Z. Luo, G. Yu, C. Zeng, and Z. Zhang, *Phys. Rev. B* **92**, 075309 (2015).
- E. Lesne, Y. Fu, S. Oyarzun, J. C. Rojas-Sánchez, D. C. Vaz, H. Naganuma, G. Sicoli, J.-P. Attané, M. Jamet, E. Jacquet, J.-M. George, A. Barthélémy, H. Jaffrès, A. Fert, M. Bibes, and L. Vila, *Nat. Mater.* **15**, 1261 (2016).
- L. Cheng, L. Wei, H. Liang, Y. Yan, G. Cheng, M. Lv, T. Lin, T. Kang, G. Yu, J. Chu, Z. Zhang, and C. Zeng, *Nano Lett.* **17**, 6534 (2017).
- P. K. Rout, E. Maniv, and Y. Dagan, *Phys. Rev. Lett.* **119**, 237002 (2017).
- A. Ariando, X. Wang, G. Baskaran, Z. Liu, J. Huijben, J. Yi, A. Annadi, A. R. Barman, A. Rusydi, S. Dhar, Y. Feng, J. Ding, H. Hilgenkamp, and T. Venkatesan, *Nat. Commun.* **2**, 188 (2011).
- D. A. Dikin, M. Mehta, C. W. Bark, C. M. Folkman, C. B. Eom, and V. Chandrasekhar, *Phys. Rev. Lett.* **107**, 056802 (2011).
- L. Li, C. Richter, J. Mannhart, and R. C. Ashoori, *Nat. Phys.* **7**, 762 (2011).
- J. A. Bert, B. Kalisky, C. Bell, M. Kim, Y. Hikita, H. Y. Hwang, and K. A. Moler, *Nat. Phys.* **7**, 767 (2011).
- C. Bell, S. Harashima, Y. Kozuka, M. Kim, B. G. Kim, Y. Hikita, and H. Y. Hwang, *Phys. Rev. Lett.* **103**, 226802 (2009).
- Z. Chen, A. G. Swartz, H. Yoon, H. Inoue, T. A. Merz, D. Lu, Y. Xie, H. Yuan, Y. Hikita, S. Raghu, and H. Y. Hwang, *Nat. Commun.* **9**, 4008 (2018).
- B. Kalisky, E. M. Spanton, H. Noad, J. R. Kirtley, K. C. Nowack, C. Bell, H. K. Sato, M. Hosoda, Y. Xie, Y. Hikita, C. Woltmann, G. Pfanzelt, R. Jany, C. Richter, H. Y. Hwang, J. Mannhart, and K. A. Moler, *Nat. Mater.* **12**, 1091 (2013).
- M. Honig, J. A. Sulpizio, J. Drori, A. Joshua, E. Zeldov, and S. Ilani, *Nat. Mater.* **12**, 1112 (2013).
- H. J. H. Ma, S. Scharinger, S. W. Zeng, D. Kohlberger, M. Lange, A. Stöhr, X. R. Wang, T. Venkatesan, R. Kleiner, J. F. Scott, J. M. D. Coey, D. Koelle, and A. Ariando, *Phys. Rev. Lett.* **116**, 257601 (2016).
- M. Mograbi, E. Maniv, P. K. Rout, D. Graf, J.-H. Park, and Y. Dagan, *Phys. Rev. B* **99**, 094507 (2019).
- K. Jiang, X. Dai, and Z. Wang, *Phys. Rev. X* **9**, 011033 (2019).
- P. A. Sobocinski, P. L. Grande, and P. Pureur, *Physica C* **506**, 87 (2014).
- N. Nagaosa, J. Sinova, S. Onoda, A. H. MacDonald, and N. P. Ong, *Rev. Mod. Phys.* **82**, 1539 (2010).
- A. Segal, M. Karpovskii, and A. Gerber, *Phys. Rev. B* **83**, 094531 (2011).
- J. Wu, A. T. Bollinger, X. He, and I. Božović, *Nature* **547**, 432 (2017).
- P. Vašek, *Supercond. Sci. Technol.* **20**, 67 (2007).
- N. Reyren, S. Gariglio, A. D. Caviglia, D. Jaccard, T. Schneider, and J.-M. Triscone, *Appl. Phys. Lett.* **94**, 112506 (2009).

- ⁴²M. H. Fischer, S. Raghu, and E.-A. Kim, [New J. Phys.](#) **15**, 023022 (2013).
- ⁴³A. Joshua, S. Pecker, J. Ruhman, E. Altman, and S. Ilani, [Nat. Commun.](#) **3**, 1129 (2012).
- ⁴⁴E. Maniv, M. B. Shalom, A. Ron, M. Mograbi, A. Palevski, M. Goldstein, and Y. Dagan, [Nat. Commun.](#) **6**, 8239 (2015).
- ⁴⁵A. E. M. Smink, J. C. de Boer, M. P. Stehno, A. Brinkman, W. G. van der Wiel, and H. Hilgenkamp, [Phys. Rev. Lett.](#) **118**, 106401 (2017).
- ⁴⁶V. L. Berezinskii, *Sov. Phys. JETP* **34**, 610 (1972).
- ⁴⁷J. M. Kosterlitz and D. J. Thouless, [J. Phys. C](#) **5**, L124 (1972).
- ⁴⁸D. Josephson, [Phys. Lett.](#) **16**, 242 (1965).
- ⁴⁹P. Fleury, J. Scott, and J. Worlock, [Phys. Rev. Lett.](#) **21**, 16 (1968).
- ⁵⁰Y. Lv, Y. Dong, D. Lu, W. Tian, Z. Xu, W. Chen, X. Zhou, J. Yuan, K. Jin, S. Bao, S. Li, J. Wen, L. F. Chibotaru, T. Schwarz, R. Kleiner, D. Koelle, J. Li, H. Wang, and P. Wu, [Sci. Rep.](#) **9**, 664 (2019).